

Use of Artificial Neural Networks for Predicting Crude Oil Effect on Carbon Dioxide Corrosion of Carbon Steels

S. Hernández,^{†,***} S. Nešić,^{**} G. Weckman,^{***} and V. Ghai^{***}

ABSTRACT

The role of crude oil on carbon dioxide (CO₂) corrosion has gained special attention in the last few years because of its significance when predicting corrosion rates. However, the complexity and variability of crude oils makes it hard to model its effects, which can influence not only wettability properties but also the corrosiveness of the associated brine. This study evaluates the usefulness of artificial neural networks (ANN) to predict the corrosion inhibition offered by crude oils as a function of several of their properties that have been related in previous studies to the protectiveness of crude oils, i.e., nitrogen and sulfur contents, resins and asphaltenes, total acid number, nickel and vanadium content, etc. Results showed that neural networks are a powerful tool and that the validity of the results is closely linked to the amount of data available and the experience and knowledge that accompany the analysis.

KEY WORDS: artificial neural networks, carbon dioxide corrosion, corrosion prediction, crude oil

INTRODUCTION

Modeling the effect of crude oil in carbon dioxide (CO₂) corrosion is not an easy task. Even though many researchers have worked in the area, the complexity of

the chemical nature of crude oil makes it difficult to generalize its behavior or to develop a mechanistic model. The majority of the work that has been done in the area is either experimental or based on field data. Even though plenty is yet to be understood, there is presently a better understanding of the effect of hydrocarbons compared to a decade ago, and there is a higher awareness of the relevance of including its effect into the available prediction models.

Nowadays, most authors agree that both wettability and changes in the brine chemistry are the major ways in which crude oil affects the corrosion of carbon steels in production environments. These two effects, in turn, are a consequence of the specific chemistry of the crude oil.

Even if no definite modeling or prediction was done, the discovery that both fluid dynamics and interfacial properties playing a role in CO₂ corrosion and the differentiation made among various crude oils with different origins played an important role in enhancing our knowledge base of the effect of crude oil in CO₂ corrosion.

In 1991, Efir¹ stressed the importance of testing the effect of specific crude oils and including it in corrosion prediction and testing. He also introduced the definition of “Corrosion Rate Break” as the level of produced water in crude oil production where corrosion is accelerated and becomes a problem. He found that the corrosion rate/produced water content curves for different crude oils commonly fall into one of three general types, as shown in Figure 1. This shows that the onset of accelerated corrosion in crude oil production cannot be reliably predicted by using

Submitted for publication January 2005; in revised form, August 2005.

[†] Corresponding author. E-mail: hernse@bp.com.

* BP America Inc., Westlake 1, Room 18.134, 501 Westlake Park Blvd., Houston, TX 77079.

** Ohio University, Institute for Corrosion and Multiphase Technology, Chemical Engineering Department, 342 West State St., Athens, OH 45701.

*** Ohio University, Industrial and Manufacturing Systems Engineering, Stocker Center 280, Athens, OH 45701-2979.

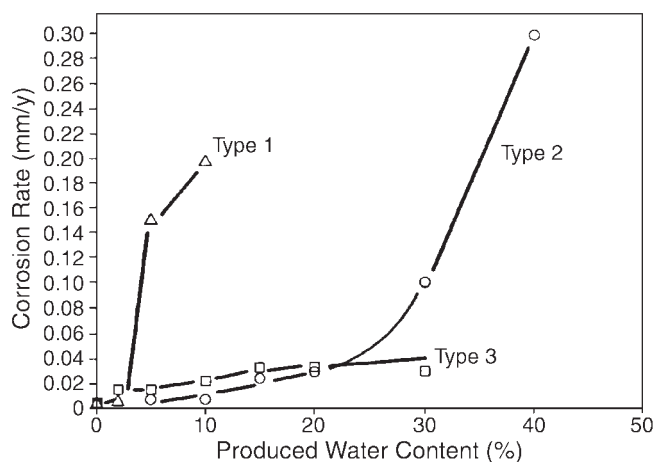


FIGURE 1. The change in corrosion rate of steel in crude oil/produced water mixtures with increasing produced water showing the three types of behavior observed.¹

a predetermined produced water level, and it also explains how different crude oils can show very different wettability properties and offer different degrees of protection.

In 1993, Smart² presented another important piece of work, relating petrophysical data and wettability properties to corrosion. Based on the work by Anderson in 1986,³⁻⁴ Smart indicated that wettability could be strongly affected by surface active compounds present in the crude oil. These surface active compounds are believed to be polar compounds containing oxygen, nitrogen, or sulfur, which are more prevalent in the heaviest fractions of crude oils such as resins and asphaltenes.

The polarity of the crude oil and the corrosion products such as iron oxide, iron carbonate, or iron sulfide also are considered a major factor in wettability. The polarity of a crude oil is described as a synergistic action of its polar and polarizable molecules, such as resins and asphaltenes and its hetero/atomic compounds: nitrogen, sulfur, and oxygen. The presence of these polar constituents could change wettability as related to corrosion by reducing the interfacial tension between water and oil and by changing the tendency of crude oil to wet the surface.

In an attempt to model the effect of crude oil, in 1993, de Waard and Lotz⁵ developed an empirical factor to be used in their widely known prediction correlation. To their expression of corrosion rate:

$$\log(V_{\text{corr}}) = 5.8 - \frac{1,710}{273 + t} + 0.67 \log(p\text{CO}_2) \quad (1)$$

a multiplier (F_{oil}) equal to one will be added when water cuts are higher than 30% and flow velocities

are bigger than 1 m/s. These critical flow rate and water percentages come from the work performed by Wicks and Fraser⁶ and Lotz, et al.,⁷ respectively. When these conditions are not met it is assumed that the steel will be oil wetted and water will be entrained in the crude oil, then the multiplier will be zero, meaning no corrosion rate. This multiplier was improved in 2001 to include different modes of water entrainment, linking API⁽¹⁾ gravity to the water-in-oil emulsion stability, which, in turn, is linked to the effect of the oil wetting of the metal. At this point the multiplier was written as:⁸

$$F_{\text{oil}} = 0.545 \frac{\alpha}{90} + 4.3WU_{\text{liq}} \left(1 + \frac{\alpha}{90}\right) \quad (2)$$

where W is the average water fraction of the liquid measured at the wellhead, U_{liq} is the liquid velocity in m/s, and α is the angle of deviation (in degrees) of the tubing from the vertical.

This factor, however, comes from fitting observed field data with corrosion rates predicted with a semi-empirical model for CO₂ corrosion,⁹ and it was exclusively developed for very light oils. Since Equation (2) can be expressed in three terms, that is:

$$F_{\text{oil}} = 4.3WU_{\text{liq}} + 0.545 \frac{\alpha}{90} + 4.3WU_{\text{liq}} \frac{\alpha}{90} \quad (F_{\text{oil}} \leq 1) \quad (3)$$

de Waard, et al., suggest that the influence of light crude oils on corrosion rates in near-liquid full systems consists of three contributions, so they tried to link each of these contributions to a specific "mode" of entrainment.¹⁰ They defined three modes of water entrainment: Mode I being water in oil emulsion, and Modes II and III occurring when water separates from the crude oil phase. In Mode II conditions are such that the water phase can remain stationary at certain locations (with oil flowing around it) while in Mode III water will move with the fluid, thus wetting the steel intermittently.

Based on the results from Craig¹¹ and using 10% water as an indicator of the emulsion breakpoint, they derived a relationship between the API gravity and the emulsion breakpoint:

$$W_{\text{break}} = -0.0166\text{API} + 0.83 \quad 50 > \text{API} > 20 \quad (4)$$

W_{break} is regarded as an indication of the interfacial tension between the crude oil and the water: the lower this tension is, the higher the amount of water is, which can be present as an emulsion in the oil. When the interfacial tension between oil and water is low, the tension will also be lower, resulting in a better wetting of the steel by the oil, thereby reducing the rate of corrosion.

This approach links oil wetting properties with API gravity of the oil. However, it remains an empiri-

⁽¹⁾ American Petroleum Institute (API), 1220 L St. NW, Washington, DC 20005.

cal correlation built on limited field data and does not consider the influence of crude oil properties, which can affect the stability of water in oil dispersions.

More recently, in 2004, a new approach was presented by Cai, et al.,¹² where a criterion for forming stable water-in-oil dispersed flow was proposed as the mean for calculating a critical velocity for water entrainment in oil-water pipe flows. To account for the complexity of the hydrodynamics and to extract a valid criterion for water separation and entrainment, Cai, et al.,¹² followed Brauner's¹³ and Barnea's¹⁴ proposals. Two main physical properties, the maximum droplet size, d_{\max} , related to breakup and coalescence, and critical droplet size, d_{crit} , related to settling and separation are compared to deduce this criterion. Since water is entrained by the flowing oil phase in the form of droplets, it is essential to know the maximum droplet size, d_{\max} , that can be sustained by the flow without further breakup. In dilute water-in-oil dispersion d_{\max} evolves from a balance between the turbulent kinetic energy and the droplet surface energy.

Droplets larger than a critical droplet size, d_{crit} , separate out from the two-phase flow dispersion, either due to gravity forces predominant in horizontal flow, or due to deformation and "creaming" typical for vertical flow. A critical droplet diameter, d_{cb} , above which the separation of droplets due to gravity takes place can be found via a balance of gravity and turbulent forces.¹⁵

The final criterion for entrainment emerges. The transition from stratified flow to stable water-in-oil dispersion takes place when the oil phase turbulence is intense enough to maintain the water phase broken up into droplets not larger than d_{\max} , which has to be smaller than the a critical droplet size d_{crit} , causing droplet separation. The transition criterion is then:¹³

$$d_{\max} \leq d_{\text{crit}} \quad (5)$$

In this model oil density was found to affect the critical velocity significantly, while surface tension and viscosity had smaller effects. The critical velocity increases water cuts.

The models described above primarily address the water wetting (entrainment and separation) issue. The question remains, however, about what it is that makes various crude oils affect corrosion differently even when tested at the same hydrodynamic conditions. Indeed, there must be something going beyond the entrainment/separation issue.

In a previous work presented by Hernández, et al., in 2002,¹⁶ an insight was given into the variables in crude oil composition that could be playing a major role in the corrosion inhibition offered by crude oils. In that work, a statistical analysis was performed with several Venezuelan crude oils evaluated experimentally under the same conditions. Crude oils were separated in two groups: paraffinic and asphaltenic,

depending on their distribution of saturates, aromatics, resins, and asphaltenes (SARA), and the effect of basic chemical and physical properties of crude oils were evaluated using multiple linear regression analyses. The variables evaluated included:

- SARA analysis
- API density
- total nitrogen
- sulfur content
- total acid number (TAN)
- concentrations of vanadium and nickel
- % crude oil

The type of crude oil, either asphaltenic or paraffinic, and its concentration were found to be significant parameters when evaluating crude-inhibiting effects. For asphaltenic crude oils, having more than 3% of asphaltenes in their composition, the parameters influencing the most at low crude oil concentrations were the sum of resins + asphaltenes, and sulfur content. At high concentrations, the effect of sulfur content was not significant and the sum of resins and asphaltenes dominates the inhibiting process.

In this case, the inhibiting capacity, defined as the ratio between corrosion rates with and without crude oil present, was described by the following equation:

$$\begin{aligned} \text{Inhibiting Capacity (asphaltenic)} = \\ 0.48 + 0.004 (\% \text{crude oil}) + 0.0048 (\% \text{resin} + \\ \% \text{asphaltenes}) + 0.0436 (\text{S}) \end{aligned} \quad (6)$$

For those crude oils considered as paraffinic, the variables with the highest influence were total nitrogen content, resins, and asphaltenes. At low crude oil concentrations, nitrogen was found to be the most significant parameter, indicating that the inhibition process can be related to the adsorption of nitrogen-based compounds at low concentrations. At higher oil concentrations, nitrogen content becomes less significant and the inhibiting capacity could be related to the formation of stable emulsions, as a result of the presence of polar functional groups found in the resin fraction.

The inhibiting capacity of paraffinic crude oils was described by:

$$\begin{aligned} \text{Inhibiting Capacity (paraffinic)} = \\ -0.230 + 0.0026 (\% \text{crude oil}) + 0.0576 (\% \text{resin}) + \\ 0.000844 (\text{N}) - 0.333 (\% \text{asphaltenes}) \end{aligned} \quad (7)$$

The results from this model are plotted in Figure 2. The correlation coefficient (R-square) values, however, were of the order of 50%, which suggested that the relationship between the predictor and the response was not really linear and that more sophisticated analysis tools should be used. This led to the use of an artificial neural network (ANN) to analyze the com-

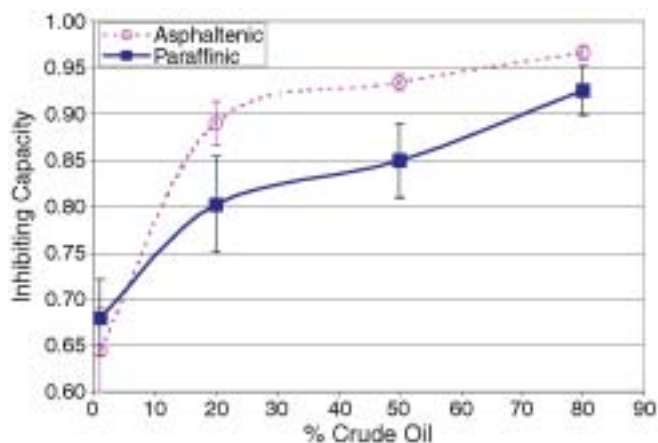


FIGURE 2. Variation of the inhibiting capacity with crude oil content for asphaltenic and paraffinic crude oils.¹⁵

plex nature of crude oils and its relationship to the inhibition.

Neural Networks as a Modeling Tool to Predict Corrosion

An ANN is an intelligent, data-driven modeling tool that is able to capture and represent complex and nonlinear input/output relationships. ANN are massively parallel, distributed processing systems that can continuously improve their performance via dynamic learning. ANN are used in many important applications, such as function approximation, pattern recognition and classification, memory recall, prediction, optimization, and noise-filtering. ANN are suited for applications involving complex systems. They are used in many commercial products such as modems, image-processing and recognition systems, speech recognition software, data mining, knowledge acquisition systems, and medical instrumentation, etc.¹⁷⁻²⁰ A key advantage of the ANN is its ability to learn, recognize, generalize, classify, and interpret incomplete and noisy inputs (data). The ANN can acquire information/knowledge about a given process through data in the training phase. This information is then stored in numerical form within the weights. ANN have proven to be powerful tools for data exploration with the capability to discover previously unknown dependencies and relationships in data sets. In cases where the input-output relations are mathematically complex, training data is noisy and the attributes are valuable, neural network approaches have been reported to perform favorably as opposed to other approaches.²¹⁻²²

ANN have been one of the most promising approaches to the corrosion modeling process. In recent years the field of artificial intelligence has been explored for modeling the corrosion process. An early

published application of a neural network to a corrosion problem was that of Smets and Bogaerts.²³ They developed a series of neural networks to predict the stress corrosion cracking (SCC) of Type 304 (UNS S30400)⁽²⁾ stainless steel in near-neutral solutions as a function of chloride content, oxygen content, and temperature. They found that the neural network approach out-performed traditional regression techniques. Ben-Hain and Macdonald²⁴ described the use of neural network models to predict the influence of various parameters on the acidity of simulated geological brines. The network inputs were the Na⁺ and Mg²⁺ concentration and the temperature. The predicted output was the pH value. The data set consisted of 101 points, of which 90 were used for training, with the remaining 11 retained as a test set.

Silverman and Rosen²⁵ combined artificial neural networks with an expert system to predict the type of corrosion from a polarization curve. Inputs to the networks included the passive current density, the pitting potential, and the repassivation potential, while outputs were the risks of crevice, pitting, and general corrosion. Two approaches were used: independent networks for each type of corrosion and a single combined network producing all three outputs. Trasatti and Mazza²⁶ developed a neural network for the prediction of the crevice corrosion behavior of stainless steels. The network was trained from long-term laboratory and field tests. Seventeen input variables were used with one hidden layer of five nodes.

Palakal, et al.,²⁷ developed an intelligent computational approach based on wavelet analysis and ANN to identify and quantify the corrosion damage images on panels obtained from nondestructive inspection (NDI) techniques. A K-mean classification algorithm was used to identify the corroded regions from the non-corroded regions in the panel based on the extracted features. Good accuracy was obtained in identification of the corroded segments. A back propagation neural network was used to predict the material loss due to corrosion. A good trend was observed between the predicted material loss and the experimental data. Pidaparti, et al.,²⁸ presented a study where the residual strength of the aging aircraft panels in the presence of corrosion and fatigue damage was examined. Both the residual strength and the corrosion rates were predicted using a neural network consisting of two hidden layer feed-forward architecture. Sensitivity analysis was performed for determining the impact of input variables on the output. The results obtained were in good agreement with the experimental data. A similar work was done by Bailey, et al.²⁹ They developed a model using neural networks to predict the ASTM G 34³⁰ metal corrosion rating and the resulting material loss in aging aircrafts.

Bucolo, et al.,³¹ modeled the corrosion phenomena occurring in the pulp and paper plant with a Multilayer Perceptron (MLP). In this study two predictive

⁽²⁾ UNS numbers are listed in *Metals and Alloys in the Unified Numbering System*, published by the Society of Automotive Engineers (SAE International) and cosponsored by ASTM International.

models were constructed. Predictive models for both a local and a global prediction were built to allow the evaluation of the corrosion rate taking place in the stainless steel used in the ozone-bleaching devices used in the plant. Leifer and Mickalonis³² presented a model based on the pitting corrosion for the carbon steel waste tanks containing aqueous radioactive waste, used for temporary storage of spent nuclear fuel while permanent storage facilities for such materials were being prepared. The ANN was used to predict the corrosion rate. Relatively good agreement was obtained between the number of pits obtained using the ANN and the number of pits experimentally measured. In one of their other works, Leifer, et al.,³³ presented a predictive model for determining pitting corrosion vs. inhibitor concentrations and temperature for radioactive sludge in carbon steel waste tanks. In this work the levels of nitrite concentrations necessary to inhibit pitting at various temperatures were experimentally determined via electrochemical polarization and coupon immersion corrosion tests. The ANN results showed a higher accuracy in predicting the conditions at which pitting occurred as compared to the logistic regression models developed.

Haque and Sudhakar³⁴ developed a model for the prediction of corrosion-fatigue crack growth rate in dual-phase (DP) steels (primarily a low-carbon steel with micro-alloying additions of vanadium and boron) using an ANN. The training data consisted of corrosion-fatigue crack growth rates at varying stress intensity ranges for martensite contents between 32% and 76%. The ANN model used consisted of three hidden layers with back-propagation architecture. The model exhibited excellent comparison with the experimental results. Nešić and Vrhovac³⁵ developed a hybrid model combining the reliability of a mechanistic model with the flexibility of the neural network approach. The model was developed using the experimental database of Dugstad, et al.³⁶ The model architecture consisted of a single hidden layer back-propagation neural network having 66 input neurons and 51 hidden neurons. Genetic algorithms (GAs) were used for the network training. The inputs to the network were indirect, crude, or noisy parameters, called primitive descriptors, such as: t , pH, PCO_2 , Fe^{++} , HCO_3^- , and v (flow velocity of oils). Relations between these primitive descriptors were studied by introducing additional problem descriptors called evolved descriptors. The prediction ability was found to be significantly better than conventional models.

The ANN is composed of several layers of processing elements or nodes. The processing elements (PE), which contain the transfer function, are linked by connections, with each connection having an associated weight, W_i . The weight of a connection expresses the relative strength of the input data or transfer data from layer to layer and output. The ANN can appear in many configurations called architectures. These

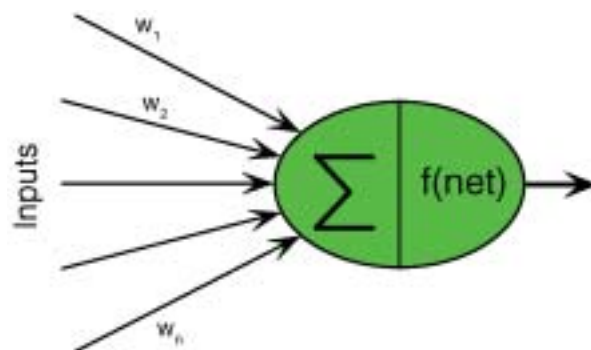


FIGURE 3. A typical PE in an ANN showing multiple inputs, one output node.²⁶

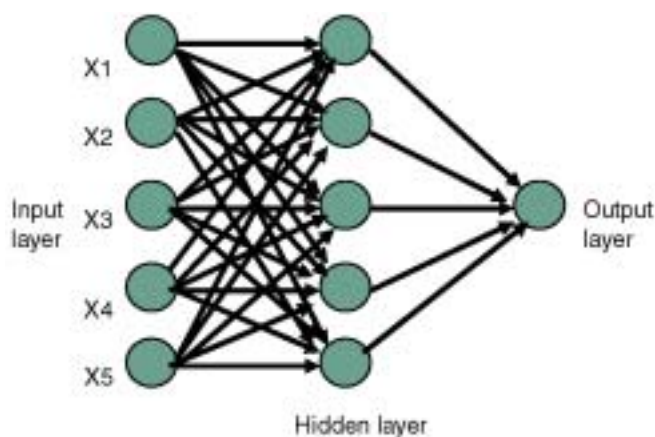


FIGURE 4. A typical ANN with five inputs, one hidden layer with five PE, and one output node.

architectures can have many different transfer functions, a different number of input PE, output PE, hidden PE, and hidden layers. Figure 3 shows a simple PE having n weights, $\{w_1, w_2, \dots, w_n\}$, and Figure 4 illustrates a typical ANN with five inputs, one hidden layer with five processing elements, and one output node.

Neural networks have two distinct phases of operation: training and testing. Typically, a number of key design parameters need to be chosen before training the network, such as: system architecture (topology), training algorithm, and number of training cycles (epochs).

During the learning phase, the network learns by adjusting the weights to correctly predict or classify the output target of a given set of input samples. With supervised learning, the network is able to learn from the input and the error (the difference between the output and the desired response). One distinguishing characteristic of an ANN is its adaptability, which requires a unique information flow design depicted in Figure 5. The performance feedback loop utilizes a cost function to provide a measure of deviation between the calculated output and the desired

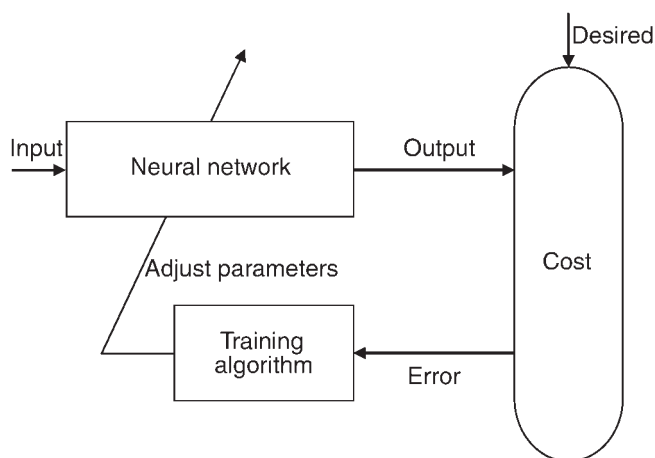


FIGURE 5. Information flow for training phase. Adapted from Principe, et al.²⁶

output. This performance feedback is utilized directly to adapt the parameters, weights, and biases, so that the system output improves with respect to the desired goal.

Once a network is trained, it is ready for the testing phase. The task of the network in the testing phase is to produce an output, given an input, based on the model or hypothesis learned during training. It is important to note that unlike in the training phase, the network parameters remain unchanged during the testing phase.

METHODOLOGY

Corrosion Data

The detailed description of the corrosion tests and results used to train the neural networks were published in a previous paper.¹⁶ Only a summary is presented below to give the reader a flavor of the procedure. Fifteen Venezuelan crude oils were evaluated (Table 1). An analysis of saturated components, aromatics, resins, and asphaltenes (SARA) was performed for each crude oil. API density ($^{\circ}$ API), total nitrogen content (N_{TOTAL}), total acid number (TAN), sulfur content (S%), vanadium (V), and nickel (Ni) were measured according to ASTM standards.

Weight-loss corrosion tests were performed on coupons exposed in autoclaves, with several crude oil-saline solution (3.5% sodium chloride [NaCl]) mixtures, simulating average conditions of well heads (72 psi CO_2 and 80°C). Water cuts were higher than 20% in all cases, and total volume inside the autoclave was always kept at 1.5 L. The test sequence was 20, 50, 80, and 99% of water (v/v), except in the cases of very heavy crude oils (Cerro Negro, Boscán y Zuata) that could only be tested at 80% and 99% water. A rotating speed of 500 rpm was kept to get a homogeneous mixture of crude oil and saline solution.

P-110 and L-80 were the steels selected for this study. Their compositions are listed on Table 2, but no significant differences were found between the two types of steel, and only P-110 results are shown in this paper. Three coupons were used for each set of testing conditions; two of them were used for corrosion rate calculations and the third for surface analysis and corrosion product characterization. Coupons were ground using a 600-grit silicon carbide (SiC) sand paper, then cleaned with acetone (CH_3COCH_3) distilled water, and dried. Their dimensions were taken and their weight was determined using an analytical balance.

The coupons were accommodated in the autoclave using the polytetrafluoroethylene (PTFE) holder. The solution was poured and the autoclave was then closed and introduced in the heater assembly. The autoclave was purged with CO_2 for 30 min to remove the air that could be inside. After deaeration, the equipment was pressurized until a pressure of 72 psi CO_2 was reached and maintained, and then the temperature was raised to 80°C in a 1-h time period. Once the conditions were found, the test was performed with a total time of 120 h. Descaling of the coupons for the calculation of corrosion rates was made according to the standard ASTM G 1-90.³⁷

After calculating corrosion rates, these were translated into inhibiting capacity by dividing the values of each test by the value obtained in blank uninhibited tests, so that:

$$\text{Inhibiting Capacity} = 1 - \frac{\text{corrosion rate}_{\text{with crude}}}{\text{corrosion rate}_{\text{blank}}} \quad (8)$$

Neural Network Development

The methodology consists of the statistical analysis of the data and development of the neural network model, and can be categorized into the following steps:

1. Preliminary analysis of the data.
2. Statistical analysis using commercially available statistical software.
3. Neural network model construction.
4. Network optimization using genetic algorithm.
5. Multiple tests runs on the selected model.
6. Sensitivity analysis to find how input variables (chemical constituents) affect the output (percentage inhibition) and their correlation with the other variables.

Step 1: Preliminary Analysis of the Data

In the preliminary analysis, various graphs and scatter plots of the data were examined to determine obvious patterns that might exist within the data. The data set included 122 records with the following minimum, maximum, and average characteristics for each variable (Table 3).

In this case no distinction was made between paraffinic and asphaltenic crude oils, as in previ-

TABLE 1
Characteristics of the Crude Oils Evaluated

	PIC4-99	PIC4-98	SBC52	VLA83	SBC36	Santa Bárbara	FUL-16	Boscán
Saturated (%)	75.4	53.8	62.2	60.6	64.6	60.5	43.2	12.4
Aromatics (%)	21.9	41	34.8	29.5	32.2	34.1	32.6	46.1
Resins (%)	2.7	5.2	3	9	3.2	5.4	17.6	29.9
Asphaltenes (%)	ND ^(A)	ND	ND	0.9	ND	ND	6.6	11.6
Sulfur (%p/p)	0.58	0.67	0.566	0.98	0.57	0.585	1.1	4.4
V (ppm)	<10	—	<10	130	—	5	125	1,059
Ni (ppm)	<10	—	<10	10	—	5	25	90
V/Ni	—	—	—	13	—	1	5	12
Total nitrogen (ppm)	819	—	34	990	628	860	3,276	6,603
TAN (KOH/g)	0.059	0.0843	0.24	0.046	0.023	0.02	0.11	1.02
°API at 60°F	35.8	31.9	42.9	33.8	30	36.2	20.7	10
Kerogen type	II (marine)	II (marine)	II (marine)	II (marine)	II (marine)	II (marine)	II (marine)	II (marine)
Maturity	Very mature	Very mature	Very mature	Mature	Very mature	Very mature	Very mature	Very mature

	Bachaquero	Menemota	Lagomedio	Pacón-Mara	Zuata	Cerro Negro	Ful29
Saturated (%)	21.1	30	47.4	41.7	13.3	13.3	41.7
Aromatics (%)	50.1	45.1	39.9	41.3	47.8	50.9	36.8
Resins (%)	19.7	16.4	10.9	11.5	28.8	23.3	18.6
Asphaltenes (%)	9.2	8.6	1.9	5.4	10.1	12.4	3
Sulfur (%p/p)	2.6	2.42	1.45	2.54	3.7	4.1	0.5
V (ppm)	409	362	232	336	458	474	48
Ni (ppm)	44	44	30	28	95	102	<10
V/Ni	9	8	8	12	5	5	—
Total nitrogen (ppm)	4,340	3,450	1,693	2,334	6,948	6,424	1,910
TAN (KOH/g)	4.78	0.74	0.14	0.40	3.35	3.67	0.49
°API at 60°F	11	20.4	30.9	27.5	8.5	8.1	15.3
Kerogen type	II (marine)	II(marine)					
Maturity	Very mature	Very mature	Very mature	Very mature	Not mature	Not mature	Very mature

^(A) ND (not detected).

TABLE 2
Chemical Composition of Carbon Steels Used (%w/w)

	C	Mn	Cr	Ni	Si	Cu	S	P
API L80	0.30	1.20	—	0.25	0.45	0.35	0.030	0.030
API P110	0.32	1.24	0.5	—	0.22	—	0.010	—

ous work, in the hope that the ANN would generate a model that could be used for all types of crude oils.

Step 2: Statistical Analysis of the Data

Multiple regression analysis was performed to determine a regression equation that would be able to explain how the model could be augmented by knowing any possible linear relationships among each of the input variables and the output. The regression equation is:

$$\begin{aligned} \% \text{Inhibition} = & 71.7 + 0.023\text{API} + 0.000086\text{total} + \\ & 0.0576\text{TAN} - 0.722\text{Saturates} - 0.714\text{Aromatics} - \\ & 0.700\text{Resins} - 0.727\text{Asphaltenes} + 0.000227\text{V} - \\ & 0.0047\text{Ni} + 0.00365\% \text{Crude oil} \end{aligned} \quad (9)$$

Details for the multiple regression is given in Table 4. The Coef is the regression coefficient for a

given variable, and SE Coef is the standard error of the coefficient. The t-value (T) is used to compare the t-value to the t-distribution to determine if a predictor is significant. The bigger the absolute value of the t-value, the more likely the predictor is significant. The p-value (P) is the probability value and it is often used in hypothesis tests to help decide whether to reject or fail to reject a null hypothesis. The p-value is the probability of obtaining a test statistic that is at least as extreme as the actual calculated value, if the null hypothesis is true. The smaller the p-value, the smaller the probability is that one would be making a mistake by rejecting the null hypothesis. A commonly used cut-off value for the p-value is 0.05. For example, if the calculated p-value of a test statistic is less than 0.05, the null hypothesis is rejected.

The p-values for the estimated coefficients of API, TAN, and crude oil are 0.000, indicating that they are significantly related to % inhibition. The p-values for

TABLE 3
Data Characteristics

Variable	Minimum	Maximum	Average
API density	8.1	36.2	24.87
Sulfur content	0.5	4.4	1.63
Total nitrogen	628	6,948	2,471.3
Total acid number	0.02	4.78	0.913
Total saturates	12.4	75.4	44.52
Aromatics	21.9	50.9	38.65
Resins	2.7	29.9	12.59
Aphaltenes	0	12.4	4.26
Vanadium	5	1,059	216.5
Nickel	5	102	28.5
%Crude oil	1	80	33.6
%Inhibition	0.153	0.999	0.8297

TABLE 4
Results of Multiple Regression

Predictor	Coef	SE Coef	T	P
Constant	71.72000	34.64000	2.07	0.041
API	0.02311	0.00546	4.24	0.000
S(%)	-0.06953	0.09460	-0.73	0.464
Total	0.00009	0.00006	1.35	0.181
TAN	0.05759	0.01581	3.64	0.000
Saturates	-0.72230	0.34640	-2.09	0.039
Aromatics	-0.71360	0.34500	-2.07	0.041
Resins	-0.70000	0.34460	-2.03	0.045
Asphaltenes	-0.72730	0.33860	-2.15	0.034
V	0.00023	0.00022	1.04	0.299
Ni	-0.00472	0.00341	-1.38	0.169
%Crude oil	0.00365	0.0040	9.05	0.00

V, Ni, Total, S% are >0.05 , indicating that these are not related to inhibition at a level of 0.05.

The R-square value obtained was 55%, which is fairly low, suggesting that the relationship between the predictor and response variables is not linear. The R-square value of 55% implies that only 55% of the variability in the output could be captured and explained by this linear model. In addition, to see if the model could be improved to better explain the relationship, the model was modified to use power transformations, which are transformations that when applied to a data set can often yield a data set that follows approximately a normal distribution. The BOX-COX and BOX-TIDWELL transformations³⁸ were performed on the original regression model. The results did not improve, reinforcing the fact that the relationship between the predictor and response variables is not linear. Finally, stepwise regression was performed to consider reducing the model size by eliminating some of the input variables (within the scope of the analysis). Once again, there was no significant improvement in the R-square value.

Step 3: Neural Network Model Construction

A number of different architectures, such as multilayer perceptron, generalized feed forward network,

modular neural network, and radial basis function, were considered for the ANN model.³⁹ The type of ANN architecture used for the analysis of corrosion inhibition for crude oil is the multilayer perceptron (MLP), so only this one will be described here. MLP are layered feed-forward networks typically trained with back-propagation (learning algorithm). MLP have been proven to be universal approximators, capable of implementing any given function through the use of various nonlinear transfer functions.⁴⁰ One of the most commonly used functions is the hyperbolic tangent function. The hyperbolic tangent function compresses a unit's net input into an activation value in the range $[-1, 1]$. A number of variations were considered and tested by varying the quantity of hidden layers and PE.

The data set was randomized and divided into training (80 records), cross validation (18 records), and test (24 records) sets.

Step 4: Network Optimization Using Genetic Algorithm

Once the MLP structure was chosen as the best model, the next step was to optimize the network architecture to select the best number of PE. Using the genetic algorithm module, the MLP with two hidden

layers (6 PE each) was shown to model the crude oil behavior, resulting in the best accuracy for predicting the inhibition rate (Figure 6).

Step 5: Multiple Tests Run on the Selected Model

After network optimization, a number of runs on the selected ANN were performed by randomizing the data, to ensure that the network was able to understand, interpret, and learn from the data. From those runs, six models (neural network Tests 1 through 6) were chosen as the best models generated. The test results of the six ANN models are shown in Table 5.

Step 6: Sensitivity Analysis

Sensitivity analysis is a method for extracting the cause and effect relationship between the inputs and outputs of the network. The network learning is disabled during this operation such that the network weights are not affected. The basic idea is that the inputs to the network are shifted slightly and the corresponding change in the output is reported either as a percentage or a raw difference. The activation control component generates the input data for the sensitivity analysis by temporarily increasing the input by a small value (dither). The corresponding change in output is the sensitivity data. Each input channel to the network was varied between its mean ± 1 standard deviation, while all other inputs were fixed at their respective mean values. Sensitivity analysis was performed for the chosen MLP network and for all the test runs for that particular model. The sensitivity was computed based on the corresponding difference (delta) in the output(s) as graphed using the Max-Min criteria of the output (inhibition). A cumulative sensitivity graph was constructed by averaging the sensitivity values for all the selected neural network test runs (Test 1 through 6).

In addition, the data was subdivided on the basis of the crude oil percentages for further analysis. The data was separated by crude oil percentage into four different groups: 1%, 20%, 50%, and 80%. A sensitivity analysis was also performed on these groups. Based on the results, similar behavior patterns were noted between the 1% and 20% crude oil data and similarly between the 50% and 80% crude oil data analyses. The similar groups were combined (1% and 20%) and (50% and 80%), and another sensitivity analysis was performed to see if there were similarities between low or high crude oil concentrations.

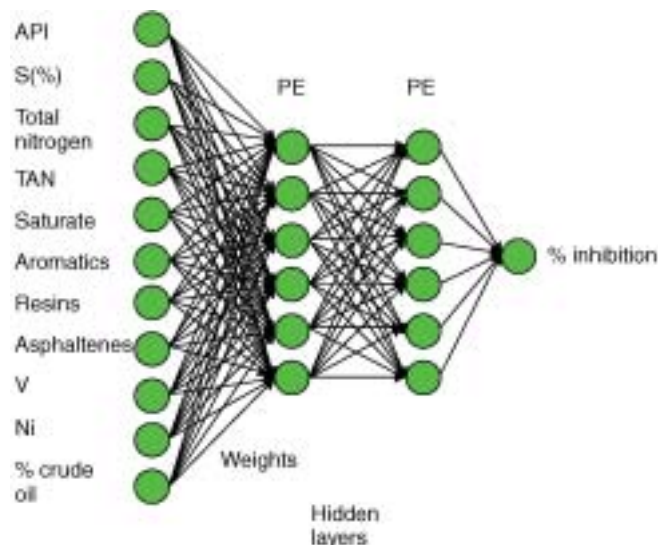


FIGURE 6. MLP architecture for crude oil inhibition.

RESULTS AND DISCUSSION

As described in the previous section, several neural network tests were performed and the sensitivity about the mean for each case was calculated. Figures 7 through 9 show examples of the results (neural network Test 6). For this particular example the R value was 0.967, and as can be seen from Figure 7 the prediction of the neural net is really accurate. From the sensitivity graph (Figure 8) it can be inferred that the variables having the greatest influence in the response were crude oil percentage (%crude oil), Ni content, API gravity, and total nitrogen, in that order. It is important to stress that the results shown here are representative of the data from these experiments, related to a sample of Venezuelan crude oils only. The results are not intended to be taken as universal until the model is completely developed and additional data are used to calibrate it.

Figures 9 through 19 show the separate sensitivity for each variable. According to this neural network test an increase in %crude oil will cause an increase in the inhibiting capacity (Figure 9). Nickel content seems to diminish the inhibiting capacity (Figure 10). API (Figure 11) and total nitrogen (Figure 12) seem to improve corrosion inhibition. Nickel in crude oils can be seen as a measure of the metal/porphyrin complex compounds containing either nickel or vana-

TABLE 5
Test Results of ANN Models

Model	1	2	3	4	5	6
Mean squared error (MSE)	0.0026	0.0031	0.0023	0.0015	0.0042	0.0035
Mean absolute error (MAE)	0.0344	0.0422	0.0347	0.0266	0.0377	0.0403
r ²	0.976	0.955	0.979	0.916	0.948	0.967

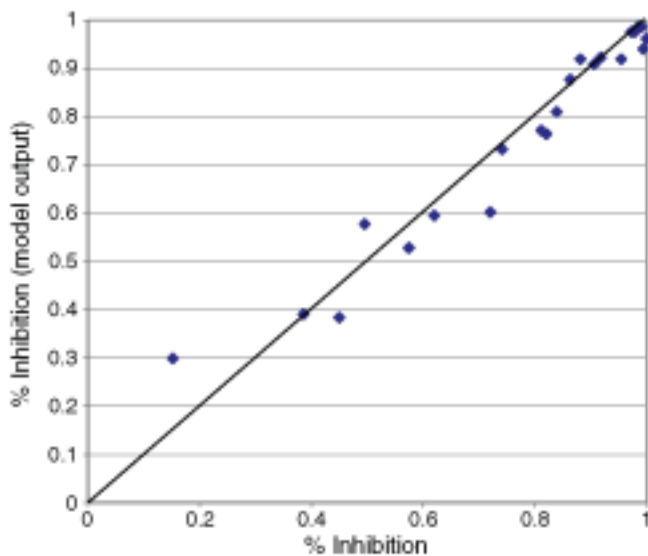


FIGURE 7. Actual vs. predicted inhibition for neural network Test 6.

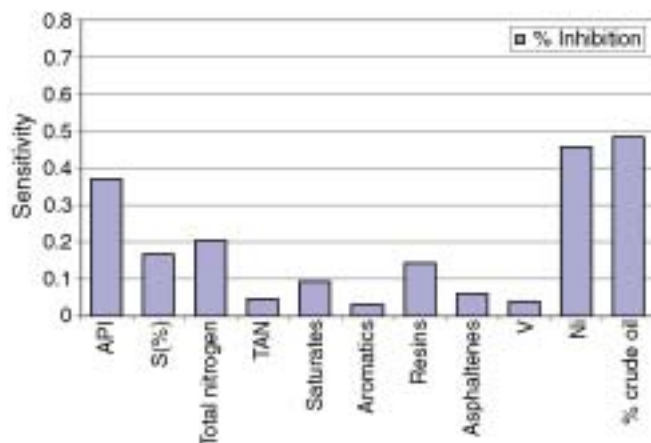


FIGURE 8. Sensitivity about the mean for Test 6.

dium, and there has been evidence indicating that these compounds are surface active and could help increase the tendency of the crude oil to wet the surface of the metal. However, in practical application, vanadium and nickel are usually measured because these materials have serious deleterious effects on catalyst performance during refining by catalytic processes.

The effect of vanadium (Figure 13) and total acid number (Figure 14) resulted in an increase in the inhibiting capacity; however, the effect is very small as can be seen for the values in the y axis. The increased content of %S in the range tested (Figure 15) showed a decrease in the inhibiting capacity.

In regard to the SARA components of the crude oil, none showed a significant effect; however, saturates (Figure 16) were shown to decrease the inhibiting capacity as their content increased, contrary to aromatics (Figure 17), resins (Figure 18), and as-

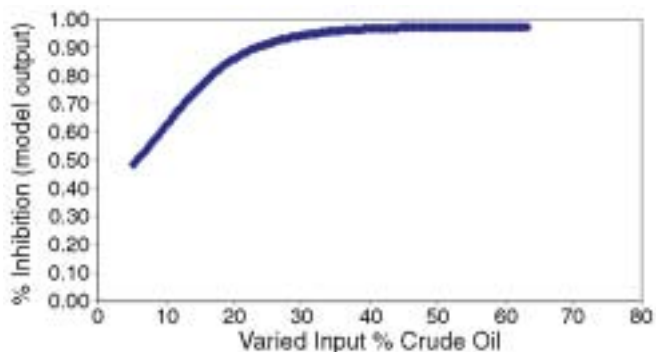


FIGURE 9. Separate sensitivity for % crude oil.

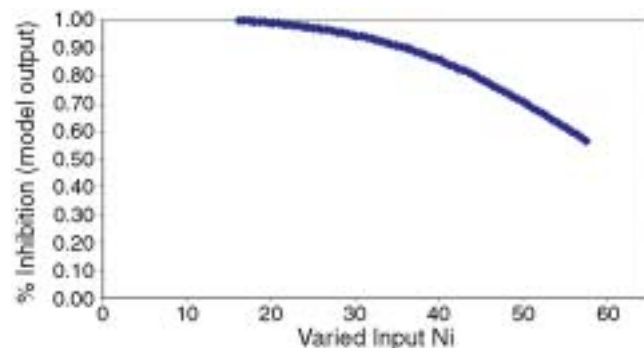


FIGURE 10. Separate sensitivity for nickel, Test 6.

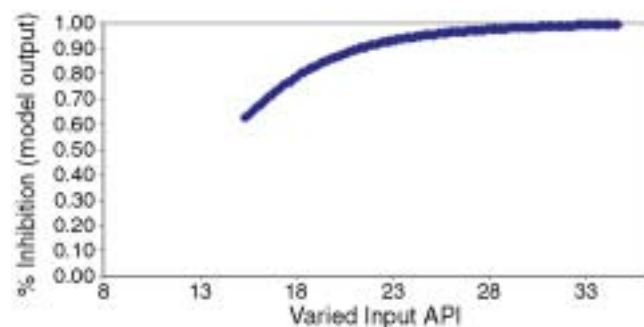


FIGURE 11. Separate sensitivity for API, Test 6.

phaltenes (Figure 19), which showed an increase in inhibition as their content increased.

Figure 20 shows the results of the neural networks in comparison with the data for the cumulative analysis from six test runs. The application of neural networks allows the user to construct the graph of crude oil vs. inhibition if all the parameters are known. As most crude oil properties are interrelated and, in turn, dependent on the origin where the crude oil comes from, it is important to know all the variables. The cumulative sensitivity, as shown in Figure 21, is the result of combining six tests and their individual sensitivities. The parameters showing the

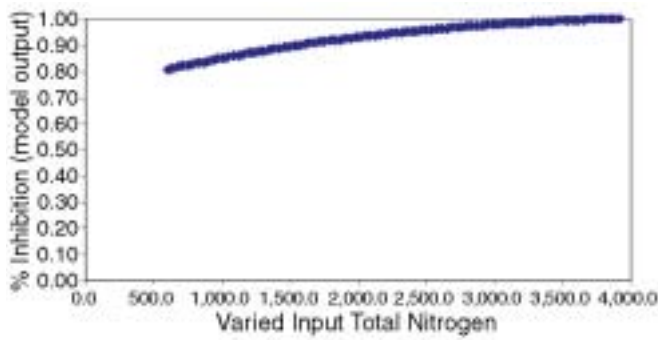


FIGURE 12. Separate sensitivity for total nitrogen, Test 6.

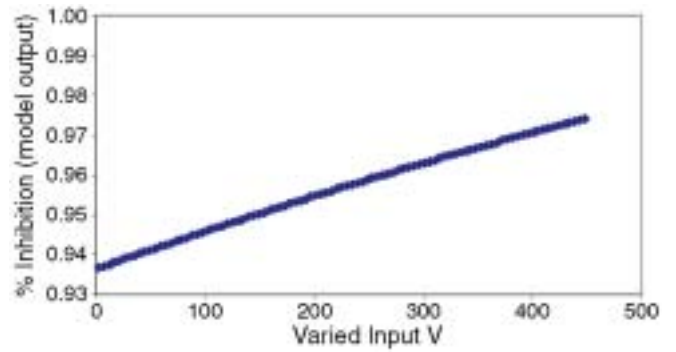


FIGURE 13. Separate sensitivity for vanadium, Test 6.

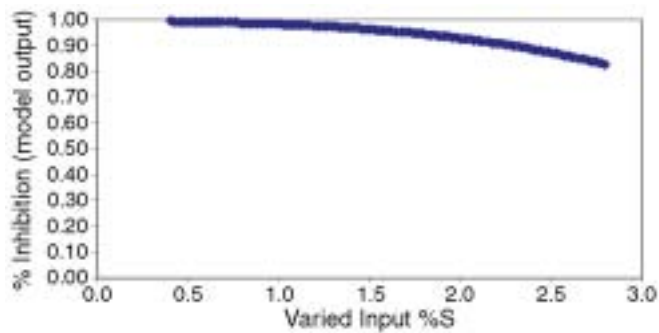


FIGURE 14. Separate sensitivity for %S, Test 6.

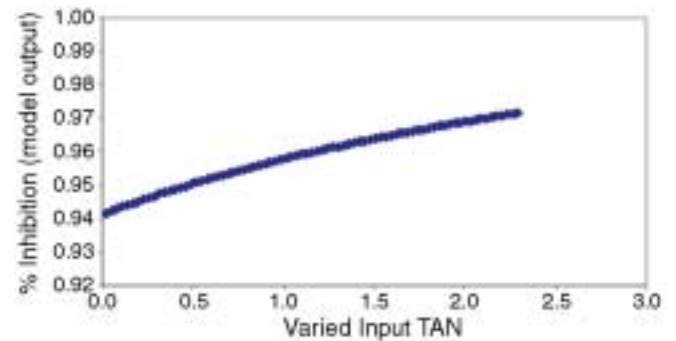


FIGURE 15. Separate sensitivity for TAN, Test 6.

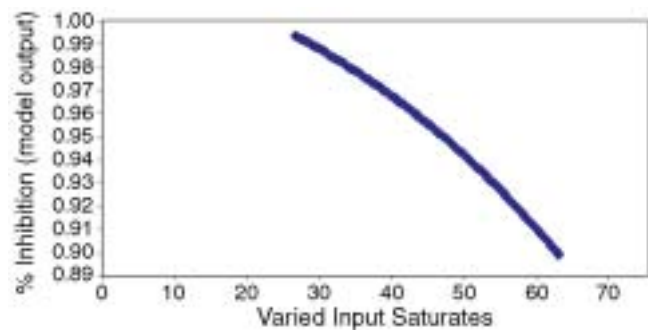


FIGURE 16. Separate sensitivity for saturates, Test 6.

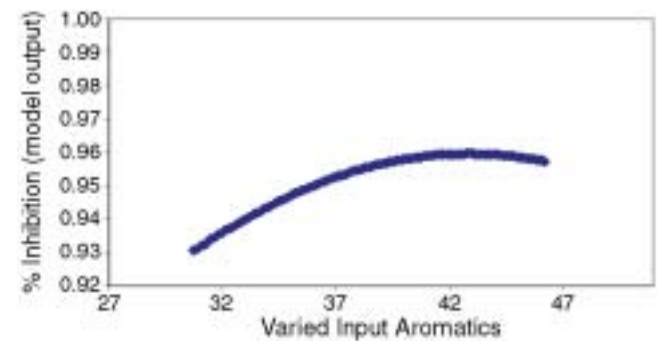


FIGURE 17. Separate sensitivity for aromatics, Test 6.

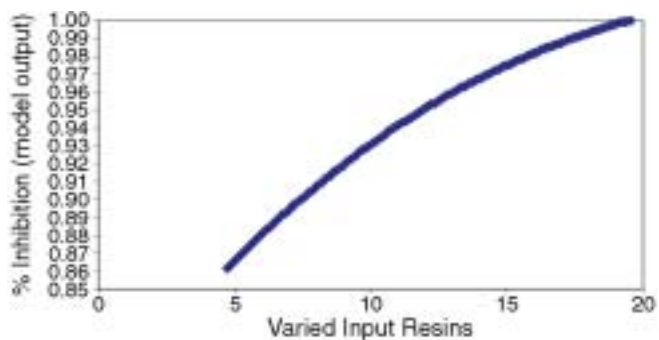


FIGURE 18. Separate sensitivity for resins, Test 6.

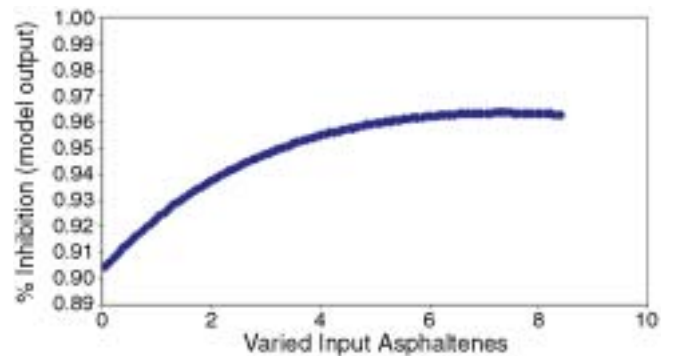


FIGURE 19. Separate sensitivity for asphaltenes, Test 6.

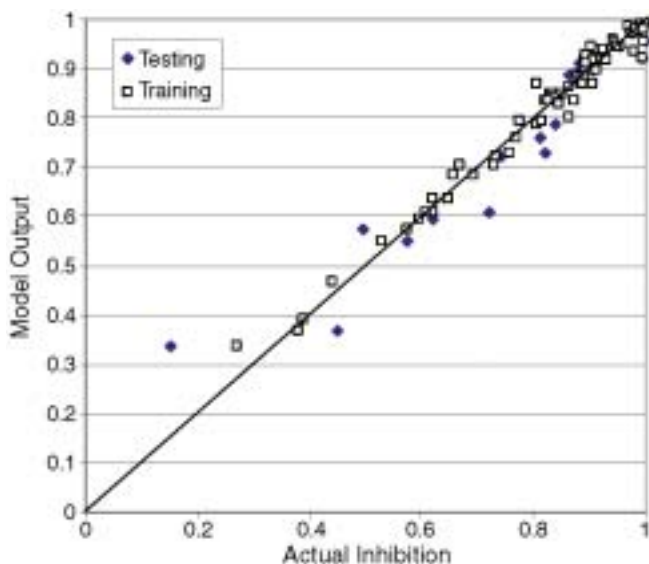


FIGURE 20. Neural network model results vs. actual data.

highest influence were %crude oil, nickel content, API degree, and TAN, in that order.

The tendency of %crude oil vs. inhibition was clear in both the data and the model. An increase in crude oil content increases the degree of corrosion protectiveness by the crude oil. With API density, even if the data is scattered, the model predicts an increase in inhibition as API increases, implying lighter crude oils providing higher values of inhibiting capacities. Regarding the nickel content, the effect was persistent through all the analysis, while it was not obvious in the data. In the ranges tested, of the 5-ppm to 110-ppm nickel, an increase in nickel content decreases the ability of the crude oil to provide inhibition. This effect is contradictory to what would be expected if one thinks of nickel as related to metal-

lic complexes that could help change interfacial properties between water and crude oil, thus helping water to get entrained and increasing crude oil wettability.

To see if this effect was repeatable, separated sensitivity analyses were performed for the various crude oil contents evaluated: 1, 20, 50, and 80%.

—For 1% crude oil (Figure 22) the model tends to predict a higher inhibiting capacity than the real measured values, but the R value is still considerably high, 0.963. Nickel appears to be most significant, followed by API, sulfur content, TAN, and asphaltenes. All increase the inhibiting capacity when increased in number or concentration, except Ni.

—For 20% crude oil (Figure 23, $R = 0.998$) nickel is not that critical and the most influential variables are API, total nitrogen, resins, and TAN. Saturates seem to have a detrimental effect.

—For 50% crude oil (Figure 24, $R = 0.960$) the four variables with the highest sensitivity are nickel, vanadium, aromatics, and sulfur. Nickel and aromatics decrease the value of inhibiting capacity as their content increases. If only positive effects are considered, then V, %S, asphaltenes, and resins show the highest influence.

—For 80% (Figure 25, $R = 0.990$) nickel and vanadium showed the highest sensitivities, in both cases producing a decrease in the inhibiting capacity as their content increases. Asphaltenes follow and then aromatics, the latter also having an inverse relationship. Note that sensitivity values are a lot higher for the first two cases.

An interesting result from the model is that it pointed out notably different behaviors when the crude oil concentration changed. By putting together the data for low concentrations (1% and 20%, Figure

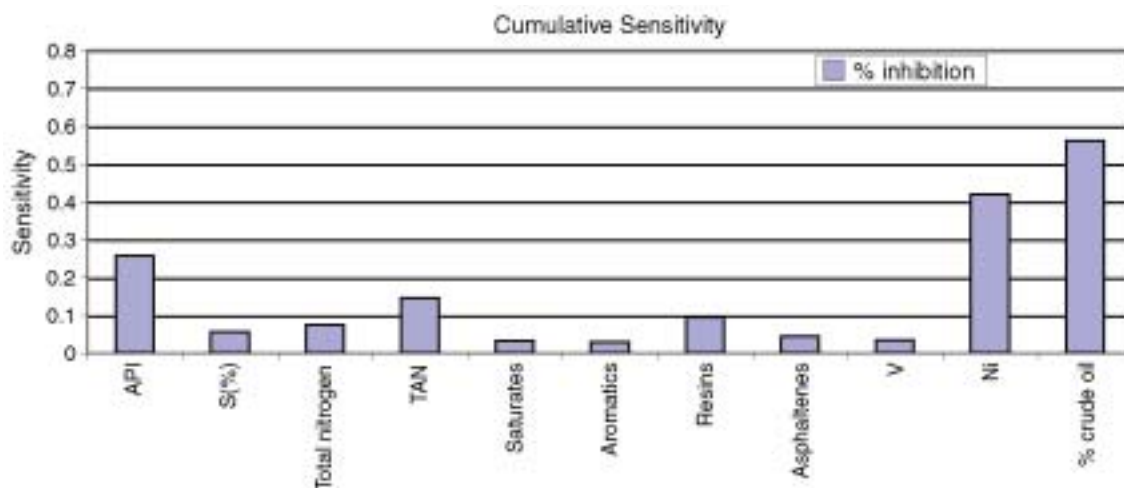


FIGURE 21. Cumulative sensitivity graph.

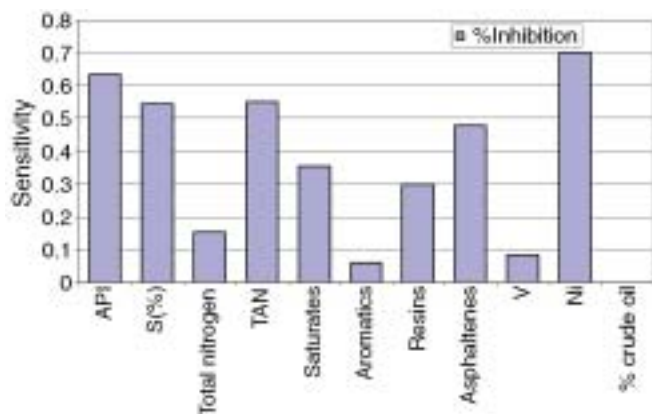


FIGURE 22. Sensitivity about the mean for 1% crude oil concentration.

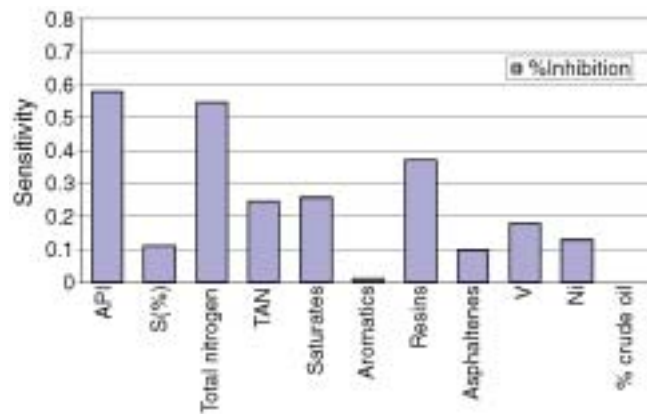


FIGURE 23. Sensitivity about the mean for 20% crude oil concentration.

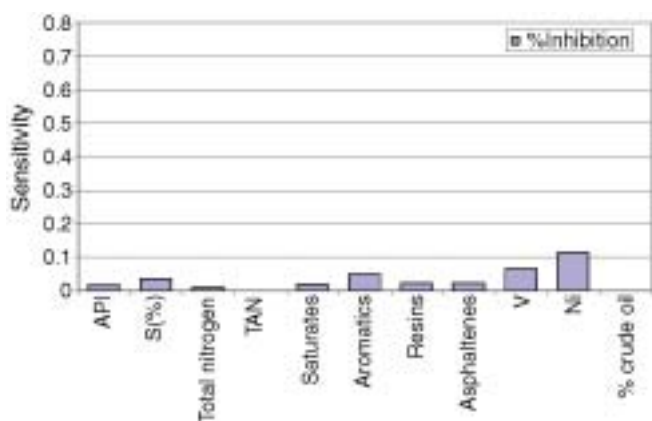


FIGURE 24. Sensitivity about the mean for 50% crude oil concentration.

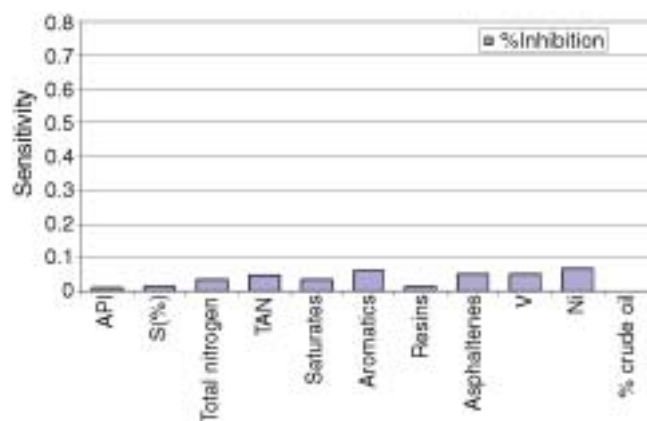


FIGURE 25. Sensitivity about the mean for 80% crude oil concentration.

26) and the data for higher concentrations (50% and 80%, Figure 27), and looking at the sensitivities, it can be concluded that at higher concentrations the presence of crude oil per se (coverage) has the greatest influence and the effects of different variables are not as relevant. At low crude oil concentrations the sensitivities are a lot higher (up to 0.8), indicating that inhibition is not as much related to the amount of crude oil but to the presence of oil or a combination of the two.

According to the model, for most cases, nickel content seems to have a great effect in decreasing the % inhibition provided by crude oil. From the scientific point of view, no explanation can be offered regarding the effect of nickel unless more experimentation is performed.

If we now return to the multiple regression analysis, it was seen that most of the input variables are highly correlated, which is actually expected based on knowledge about crude oil chemistry. The following relationships were found by analyzing the data on this paper (graphs are not shown for space limitations):

- Increased amounts of the aromatic compound result in an increase in density (API density), whereas an increase in saturated compounds results in a decrease in API density.
- Lower API crude oils tend to have higher sulfur contents (%S), asphalt content (asphaltenes and resins), and are associated with higher nitrogen contents.
- As % sulfur increases so does nickel, and both nickel and vanadium tend to decrease as API increases.

These highly correlated variables made it hard for the neural network to pick up sensitivities; however, by combining the multiple regression results with the neural network results it can be inferred that at low oil concentrations API could be used as the leading variable in the inhibition process. On the other hand, all variables evaluated will be affecting inhibition to some degree, so all of them would have to be measured and further analysis will have to be performed to see if these covariations can be systematically predicted.

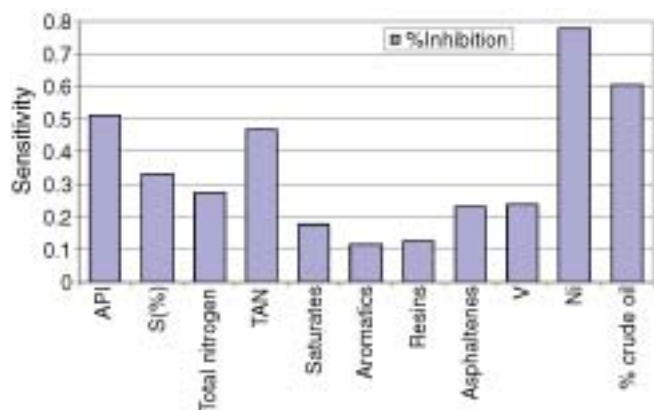


FIGURE 26. Sensitivity about the mean for 1% and 20% combined.

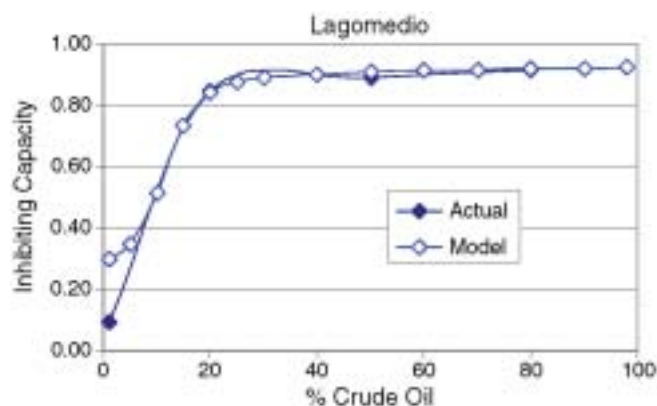


FIGURE 28. Prediction of the neural network when all variables are known.

To illustrate this point, Figure 28 shows an example of the response of the neural network when all input variables are known, while Figure 29 shows an example of a crude oil where only four variables were known (resins, asphaltenes, nickel content, and sulfur) and the rest were deduced from rough approximations using the relationships found from the multiple regression analysis. When all variables are known, the response is more accurate, as expected. However, the response in the second case is not bad, indicating that by doing a profound analysis of these relationships the model could be improved and the number of inputs could be reduced.

CONCLUSIONS

- ❖ Based on experimental data from Venezuelan crude oils an effective neural network model was developed that can predict the ability of a crude oil to provide corrosion protectiveness in a CO₂ environment.
- ❖ Provided that the model is fed with enough data from crude oils with different origins, the model would have the capability of creating the curve of %crude

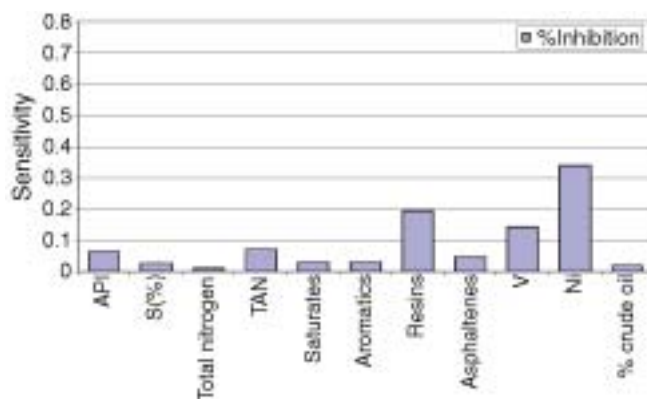


FIGURE 27. Sensitivity about the mean for 50% and 80% combined.

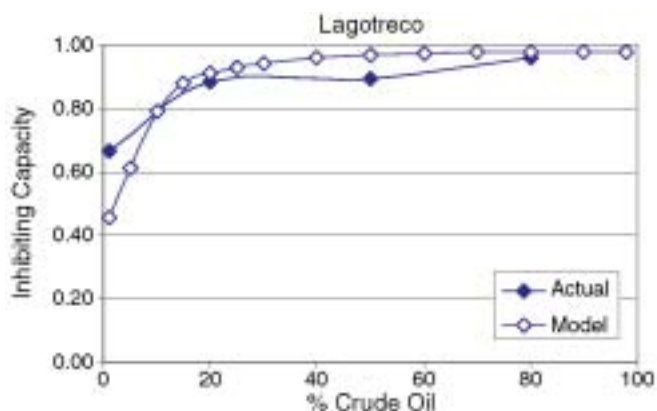


FIGURE 29. Prediction of the neural network by knowing four variables and deducing the others from the linear relationships found with the multiple regression analysis.

oil vs. corrosion rate for a given crude oil by knowing some of its physical and chemical properties, most of them routinely measured.

- ❖ Sensitivity analyses were performed to extract the variables having the highest effect on the response. Most of the trends noticed in the experimental data were captured by the network. However, the indicated correlations between the variables could not always be explained and could lead to dubious interpretations. More research is needed to expand both the experimental database and the modeling capability, with a goal to generate the knowledge necessary to determine the factors governing the effect of crude oil in CO₂ corrosion.

FUTURE WORK WITH ANN

ANN act like "black boxes" in the sense that relationships are encoded incomprehensibly as weight vectors within the trained network. Although ANN have proven to be empirically successful, they are generally treated as numerical enigmas, often gen-

erating incomprehensible and hard-to-understand models. They cannot easily support the generation of scientific theories unless these relationships can be explained in a comprehensible form to aid in the process of prediction. Generally, these models are difficult to understand because the processing in a neural network occurs at the sub-symbolic level as numerical estimation and manipulation of network parameters. Therefore, it is not always possible to directly translate these large sets of real valued parameters into symbols or concepts that have semantic significance. Thus, the inability to provide an end-user with the capability to explain the ANN have generally been recognized as the most significant obstacles to the more widespread application of ANN.

The goal of a knowledge extraction algorithm is to translate this neural network model into an explicit symbolic form. Knowledge extraction can enhance the capabilities of an ANN by developing rules based on the assigned weights. The knowledge embedded within the trained ANN in the form of weights needs to be extracted and expressed as a set of rules. Basically, knowledge is acquired during the training phase and is then encoded within the network architecture, the activation function associated with each layer, and the set of numerical weights. Knowledge extraction is based on the behavior of the neurons within the ANN. A significant amount of research has been expended in recent years to develop techniques for the extraction of knowledge from trained ANN. Key methods include the M-of-N algorithm, validity interval analysis (VIA), genetic algorithm approach, the TREPAN algorithm to Fuzzy ARTMAP system, and other approaches.⁴¹⁻⁴⁶

For future research, the plan is to use a few techniques such as TREPAN and C4.5 (Decision Tree algorithms) where the resulting decision tree approximates the network. This approach would add to and refine the role of crude oil in CO₂ corrosion by approaching the problem from a knowledge-based perspective. Corrosion inhibition, as noted earlier in this paper, is a function of several factors related to the protectiveness of crude oils. Incorporating this extracted knowledge into a model will have many advantages in improving the accuracy and ability in predicting CO₂ corrosion behavior. These decision tree algorithms could aid in further understanding the relationships between the input variables and inhibition with crude oils. By extracting knowledge into a comprehensible form, further relationships between input and output variables can be explored and can be used to support the generation rule-based systems. These extracted comprehensible rules aid in developing a more usable prediction tool and enhance the understanding of the CO₂ corrosion process. Extracting knowledge from a neural network-based model and then converting it into a comprehensible form is what makes this future research so useful. This knowledge

will be used to further develop a hybrid (theoretically and empirically based) model for better prediction of CO₂ corrosion rates.

REFERENCES

1. K.D. Efirid, "Preventive Corrosion Engineering in Crude Oil Production," Offshore Technology Conference (OTC), paper no. 6599 (Houston, TX: OTC, 1991), p. 355-362.
2. J.S. Smart, "Wettability—A Major Factor in Oils and Gas System Corrosion," CORROSION/93, paper no. 70 (Houston, TX: NACE International, 1993), p. 70/1-70/15.
3. W. Anderson, *J. Petrol. Technol.* 10 (1986): p. 1,125-1,144.
4. W. Anderson, *J. Petrol. Technol.* 11 (1986): p. 1,246-1,262.
5. C. de Waard, U. Lotz, "Prediction of CO₂ Corrosion of Carbon Steel," CORROSION/93, paper no. 69 (Houston, TX: NACE, 1993), p. 69/1-69/17.
6. M. Wicks, *J.P. Fraser, Mater. Perform.* 14, 5 (1975): p. 9.
7. U. Lotz, L. van Bodegom, C. Ouwehand, "The Effect of Type of Oil and Gas Condensate on Carbonic Acid Corrosion," CORROSION/90, paper no. 41 (Houston, TX: NACE, 1990), p. 635-645.
8. C. de Waard, L. Smith, P. Bartlett, H. Cunningham, "Modelling Corrosion Rates in Oil Production Tubing," EUROCORR 2001, paper no. 254 (Lake Garda, Italy: The European Corrosion Congress, European Federation of Corrosion, 2001), p. 1-8.
9. C. de Waard, U. Lotz, A. Dugstad, "Influence of Liquid Flow Velocity on CO₂ Corrosion: A Semi-Empirical Model", CORROSION/95, paper no. 128 (Houston, TX: NACE, 1995), p. 128/1-128/15.
10. C. de Waard, L. Smith, B.D. Craig, "The Influence of Crude Oil on Well Tubing Corrosion Rates," EUROCORR 2001, paper no. 174 (Lake Garda, Italy: The European Corrosion Congress, European Federation of Corrosion, 2001), p. 1-8.
11. B. Craig, "Predicting the Conductivity of Water-in-Oil Solutions as a Means to Estimate Corrosiveness," CORROSION/98, paper no. 54 (Houston, TX: NACE, 1998), p. 657.
12. J. Cai, S. Nešić, C. de Waard, "Modeling of Water Wetting in Oil-Water Pipe Flow," CORROSION/2004, paper no. 04663 (Houston, TX: NACE, 2004), p. 1-19.
13. N. Brauner, *Int. J. Multiphase Flow* 27 (2001): p. 885-910.
14. D. Barnea, *Int. J. Multiphase Flow* 11 (1987): p. 1-12.
15. R.S. Brodkey, *The Phenomena of Fluid Motions* (Reading, MA: Addison-Wesley, 1969).
16. S. Hernández, S. Duplat, J.R. Vera, E. Barón, "A Statistical Approach for Analyzing the Inhibiting Effects of Different Types of Crude Oil in CO₂ Corrosion of Carbon Steel," CORROSION/2002, paper no. 02293 (Houston, TX: NACE, 2002), p. 1-15.
17. T. Efraim, E.A. Jay, T.P. Liang, R.V. McCarthy, *Decision Support Systems and Intelligent Systems* (Upper Saddle River, NJ: Prentice Hall, 2001).
18. Y. LeCun, B. Boser, J.S. Denker, D. Henderson, R.E. Howard, W. Hubbard, L.D. Jackel, *Neural Computation* 1 (1989): p. 541-551.
19. D.A. Pomerleau, "ALVINN: An Autonomous Land Vehicle in a Neural Network," Technical Report CMU-CS-89-107, Morgan Kaufmann Publishers, Inc., January 1989.
20. A.H. Waibel, *Neural Computation* 1 (1989): p. 39-46.
21. S.B. Thurn, "Extracting Provably Correct Rules from Artificial Neural Networks," Technical Report IAI-TR-93-5, University of Bonn, January 1993.
22. G.G. Towell, J.W. Shavlik, *Mach. Learning* 13 (1993): p. 71-101.
23. H.M.G. Smets, W.F.L. Bogaerts, *Mater. Perform.* 31 (1992): p. 64-67.
24. M. Ben-Hain, D.D. Macdonald, *Corros. Sci.* 36 (1994): p. 385-393.
25. D.C. Silverman, E.M. Rosen *Corrosion* 48 (1992): p. 734-745.
26. S.P. Trasatti, F. Mazza, *Br. Corros. J.* 31 (1996): p. 105-112.
27. M.J. Palakal, R.M. Pidaparti, S. Rebbapragada, C.R. Jones, *AIAA J.* 39, 10 (2001): p. 1,936-1,943.
28. R.M. Pidaparti, A. Jayanti, M.J. Palakal, *J. Aircr.* 1, 39 (2002): p. 175-180.
29. R.A. Bailey, S. Jayanti, R.M. Pidaparti, M. J. Palakal, "Corrosion Prediction in Aging Aircraft Materials Using Neural Networks," Proc. 41st AIAA/ASME/ASCE/ACS Conf. on Struct. and Struct. Dynamics and Mater., April 3-6, 2000 (Reston, VA/New York, NY/Washington DC: AIAA & ASCE/ASME/ACS, 2000).
30. ASTM G 34-01, "Standard Test Method for Exfoliation Corrosion Susceptibility in 2XXX and 7XXX Series Aluminum Alloys (EXCO Test)," in *Annual Book of ASTM Standards* (West Conshohocken, PA: ASTM International, 2005).

31. M. Bucolo, L. Fortuna, M. Nelke, A. Rizzo, T. Sciacca, "Prediction Model for the Corrosion Phenomena in Pulp and Paper Plant," in *Control Engineering Practice*, 10 (Elsevier Science North America, 2002): p. 227-237.
32. J. Leifer, J.I. Mickalonis, "Prediction of Pitting Corrosion in Aqueous Environments via Artificial Neural Network Analysis," *Proc. Artificial Neural Networks in Engineering (ANNIE) 98* (St. Louis, MO: Univ. Missouri-Rolla/IEEE Neural Networks Council, 1998).
33. J. Leifer, P.E. Zapp, J.I. Mickalonis, *J. Eng. Sci. Corros.* 55, 1 (1999): p. 31-37.
34. M.E. Haque, K.V. Sudhakar, *Int. J. Fatigue* 23, 1 (2001): p. 1-4.
35. S. Nešić, M. Vrhovac, *J. Corros. Sci. Eng.* 1 (1998): p. 211-240.
36. A. Dugstad, L. Lunde, K. Videm, "Parametric Study of CO₂ Corrosion of Carbon Steel," *CORROSION/94*, paper no. 14 (Houston, TX: NACE, 1994).
37. ASTM G 1-90, "Standard Practice for Preparing, Cleaning, and Evaluating Corrosion Test Specimens," in *Annual Book of ASTM Standards* (West Conshohocken, PA: ASTM International, 2005).
38. D.C. Montgomery, E.A. Peck, G. Vining, *Introduction to Linear Regression Analysis*, 3rd ed. (New York, NY: John Wiley and Sons, 2001), p. 186-310.
39. J.C. Principe, E.R. Euliano, W.C. Lefebvre, *Neural and Adaptive Systems: Fundamentals Through Simulations with CD-ROM*, (New York, NY: John Wiley and Sons, Inc., 1999), p. 100-172.
40. R.D. Reed, R.J. Marks, *Neural Smithing: Supervised Learning in Feedforward Artificial Neural Networks* (Cambridge, MA: MIT Press, 1998), p. 257-264.
41. L.M. Fu, "Rule Learning by Searching on Adapted Nets," *Proc. 9th National Conf. on Artificial Intelligence* (Anaheim, CA: AAAI Press, 1991), p. 590-595.
42. M.W. Craven, J.W. Shavlik, "Learning Symbolic Rules Using Artificial Neural Networks," *Proc. 10th Int. Conf. on Machine Learning* (Amherst, MA: Morgan Kaufmann, 1993), p. 73-80.
43. E. Keedwell, A. Narayanan, D.A. Savic, "Using Genetic Algorithms to Extract Rules from Trained Neural Networks," *Proc. Genetic and Evolutionary Computing Conference* (Orlando, FL: Morgan Kaufmann, 1999), p. 793.
44. C. McMillan, M.C. Mozer, P. Smolensky, "The Connectionist Scientist Game: Rule Extraction and Refinement in a Neural Network," *Proc. 13th Annual Conf. Cognitive Science Society* (Hillsdale, NJ: Lawrence Erlbaum, 1991), p. 424-430.
45. M.W. Craven, J.W. Shavlik, "Using Sampling and Queries to Extract Rules from Trained Neural Networks," *Proc. 11th Int. Conf. on Machine Learning* (New Brunswick, NJ: Morgan Kaufmann, 1994), p. 37-45.
46. G.A. Carpenter, S. Grossberg, N. Markuzon, J. Reynolds, D. Rosen, *IEEE Trans. Neural Networks* 3 (1992): p. 698-713.

ASTM International Symposium on Advances in Electrochemical Techniques for Corrosion Monitoring and Measurement

Issues a Call for Papers

Papers are invited for a Symposium on Advances in Electrochemical Techniques for Corrosion Monitoring and Measurement, sponsored by ASTM Committee G01 on Corrosion of Metals and its Subcommittee G01.11 on Electrochemical Techniques for Corrosion Monitoring. The symposium will be held May 22-23, 2007, in Norfolk, VA, in conjunction with the May 23-24, 2007, standards development meetings of Committee G01.

This symposium will cover the use of electrochemical techniques for corrosion as applied to monitoring, measurements, new test methods, and life prediction/modeling. The objective of this symposium is to provide a forum for discussing the latest advances in electrochemical techniques as they relate to the corrosion of metals.

To participate in the symposium, presenters/authors must submit the online Abstract Submittal Form, <http://www.astm.org/MEETINGS/COMMIT/G01symp.html>, and attach a 250-300 word preliminary abstract by August 4, 2006. The abstract must include a

clear definition of the objective and approach of the work discussed, pointing out material that is new, and present sufficient details regarding results. The presentation and manuscript must not be of a commercial nature nor can it have been previously published. Because a limited number of abstracts will be accepted, be sure that the abstract is complete to allow for careful assessment of the paper's suitability for this symposium. The symposium chairman, Sankara Papavinasam, will notify you in writing by October 4, 2006, of your paper's acceptability for presentation at the symposium. If the preliminary abstract is accepted, the presenter/author will be requested to submit a final camera-ready abstract several months before the symposium. The final abstracts will be distributed in an abstract booklet at the symposium.

Publication of the peer-reviewed symposium papers in the online journal, *Journal of ASTM International (JAI)*, is anticipated. JAI is an online, peer-reviewed journal for the international scientific and engineering com-

munity. You may view JAI at www.astm.org/JAI.

Once the final selection of abstracts has been approved, the ASTM staff will send you authors' instructions. Manuscripts to be peer reviewed for JAI are due at ASTM Headquarters by March 15, 2007. The corresponding author (the author who is the main contact with ASTM Headquarters) will receive a complimentary copy of his/her paper in portable document format (PDF). All published authors will have the opportunity to purchase reprints of their papers at a nominal cost.

Additional information about the symposium is available from Symposium Chairman Sankara Papavinasam, CANMET-MTL, Ottawa, ON, Canada (phone: 613/947-3603; spapavin@nrcan.gc.ca); Co-Chairman Neal S. Berke, W.R. Grace & Company Construction Products, Cambridge, MA (phone: 617/498-4827; neal.s.berke@grace.com); or Co-Chairman Sean Brossia, CC Technologies, Dublin, OH (phone: 614/761-1214; sbrossia@cctech-nologies.com).